CRISM-BASED MINERAL ABUNDANCE MAPS FOR THE OXIA PLANUM DELTA. T. Condus, Washington University in St. Louis, McDonnell Center for the Space Sciences, Department of Earth and Planetary Sciences, tcondus@wustl.edu.

Introduction: In 2023, the ExoMars Rosalind Franklin rover will land in the Oxia Planum region of Mars, an area characterized by its widespread, Noachian-aged clay-bearing deposits as detected by Observatoire pour la Minéralogie, l'Eau, les Glaces et l'Activité (OMEGA) and Compact Reconnaissance Imaging Spectrometer for Mars (CRISM) orbiter data [1, 2]. Based on absorption band comparisons and spectral unmixing experiments using CRISM data, these clay-bearing deposits most likely contain a vermiculite (Fe/Mg phyllosilicate) phase [2-4]. A prominent feature of Oxia Planum is the deltaic fan situated at the outlet of the Coogoon Valles fluvial system, which is located towards the southeastern part of the region. The delta fan deposits postdate the underlying clay-bearing deposits, and so both are believed to have formed in distinct aqueous environments [1]. Furthermore, based on spectral analyses, the delta fan deposits appear to have a mineralogy consistent with Fe-rich olivine, pyroxene, and hydrated silica [3, 5].

Although there has been much effort involving the detection of specific mineral phases in Oxia Planum, there do not yet exist detailed mineral abundance maps for this region. Preliminary mineral abundance map results are shown in this work, focusing on CRISM scene ATU00038B10 containing a large portion of the delta fan, along with a few clay-bearing deposits which have very strong D2300 spectral parameter values (Fig. 1) [6].

Methods: Using the Washington University in St. Louis pipeline [7], CRISM I/F data products are converted to single-scattering albedo (SSA) via a DISORT-generated lookup table. Specifically, DISORT is used to model radiance on instrument sensor, atmospheric gases and aerosols, and the Hapke function as the surface boundary condition for reflectance. Next, the SSA data are denoised using a maximum likelihood method approach. After being map-projected, the S and L data are coregistered to a CTX basemap through a combination of manually-selected tie points and triangulation warping using ENVI.

To build the mineral abundance maps, the CRISM scene is first downsized into roughly 3x3 pixel aggregates, to reduce the computation workload for the spectral unmixing that will follow. Then, nonlinear Hapke-based spectral unmixing is performed on a pixel-by-pixel basis using a Markov chain Monte Carlo (MCMC) method [8]. In contrast to more traditional

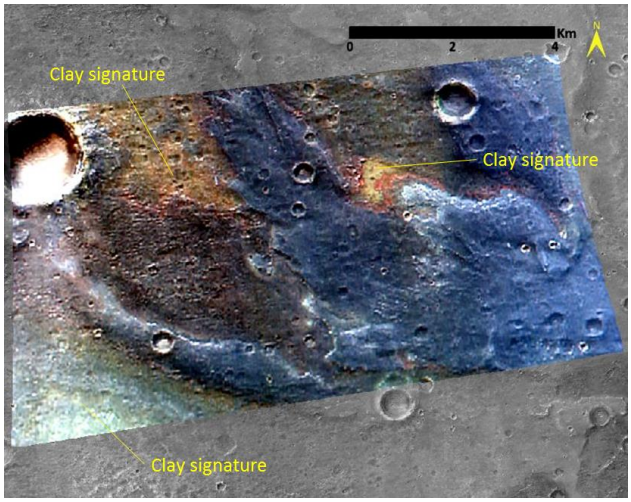

Figure 1. CRISM scene ATU00038B10, showing the Oxia Planum delta and deposits with strong clay signatures. Basemap is a CTX mosaic.

spectral unmixing techniques, MCMC computes a range of model solutions that best fit the spectral data, in terms of probability density functions (PDFs) for each endmember's abundance and grain size. The mode of each of these PDFs is the maximum a posteriori probability model (MAP), which are the abundance values that are mapped in the figures. For brevity, the distribution of the grain sizes are not shown.

A set of six endmembers are used as inputs to the MCMC algorithm, including labradorite (HS17.3B, USGS), olivine Fo50 (c1dd93, RELAB), augite (c1dl68a, RELAB), and pigeonite (c1dl09a, RELAB). Since vermiculite is a likely component of the clay-bearing deposits, it is also included as part of the ensemble (cave01, RELAB). Finally, an in-scene clay region of interest (ROI) endmember is used, as described in [4].

Results and Discussion: The mineral abundance map results are shown in Fig. 2. There is an excellent correspondence between the deposits with a strong D2300 clay signature and the high abundances for the clay ROI endmember. Vermiculite is also present as a component in the clay-bearing deposits, but more prevalent in the eastern deposit. The modeled abundances for vermiculite may be trading off with the clay ROI endmember, which could be accounting for much of the spectral shape. Interestingly, the "redder" clay deposits towards the eastern part of the scene do not contain any modeled vermiculite while containing

a significant amount of the clay ROI endmember, which indicates that it is likely composed of a different type of clay mineral compared to the "yellower" deposits. Olivine Fo50 also associates with these clay-bearing deposits, which is consistent with previous work [2-4]. These same clay-bearing deposits are devoid of basaltic minerals (labradorite, augite, and pyroxene), although it is possible that the clay ROI endmember may be accounting for these minerals in small amounts, and so they may be under-modeled.

While the RMSE values are very small for the clay-bearing deposits (indicating excellent model fits), the RMSE values are much higher for the actual delta materials. This is a consequence of using the clay ROI endmember as a component in the unmixing, which is not representative of the deltaic unit. Instead, this highlights how spectrally unique the deltaic unit is compared to the clay-bearing deposits.

Future Work: For ease of computation, the simplifying assumption of using the same set of endmembers across the entire scene was made, which is not ideal. Also, the use of in-scene endmembers may obscure the true modeled abundances of pure mineral phases. Therefore, a method to determine a proper set of pure mineral endmembers on a pixel-by-pixel basis will be developed. Additional mineral abundance maps for the larger Oxia Planum region will also be generated, where targeted CRISM data exists.

References: [1] Quantin-Nataf C. et al. (2021) *Astrobiology, 21*(3), 345-366. [2] Mandon L. et al. (2021) *Astrobiology, 21*(4), 464-480. [3] Turner S. M. R. and Bridges J. C. (2017) *LPS XLVIII,* Abstract #2228. [4] Condus T. (2021) *LPS LII,* Abstract #1670. [5] Pan L. et al. (2021) *PSJ, 2*(2), 65. [6] Viviano-Beck C. E. et al. (2014) *JGR: Planets, 119*(6), 1403-1431. [7] Politte D. V. et al. (2019) *LPS L,* Abstract #2690. [8] Lapotre, M. G. A. et al. (2017) *JGR: Planets, 122*(5), 983-1009.

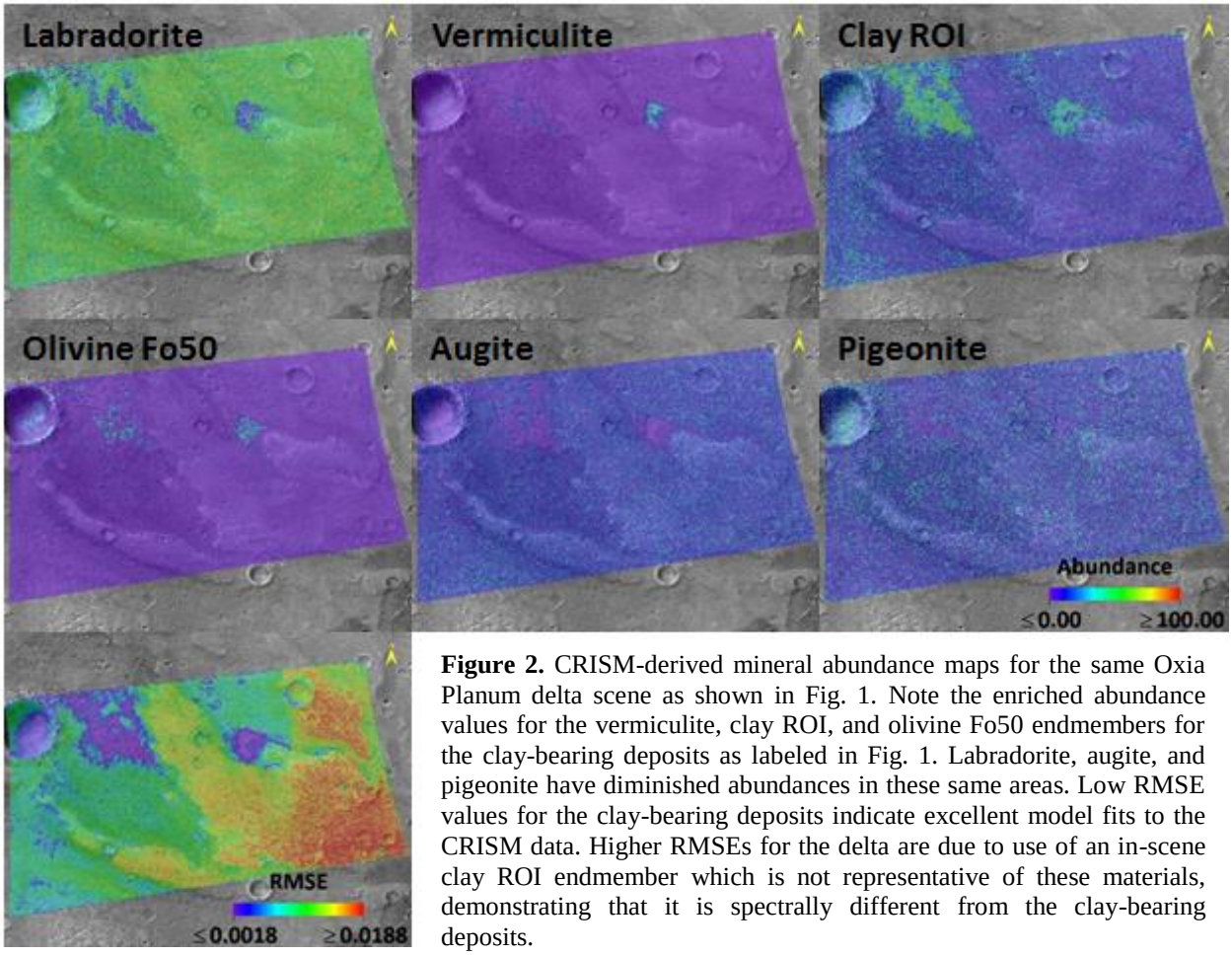

Figure 2. CRISM-derived mineral abundance maps for the same Oxia Planum delta scene as shown in Fig. 1. Note the enriched abundance values for the vermiculite, clay ROI, and olivine Fo50 endmembers for the clay-bearing deposits as labeled in Fig. 1. Labradorite, augite, and pigeonite have diminished abundances in these same areas. Low RMSE values for the clay-bearing deposits indicate excellent model fits to the CRISM data. Higher RMSEs for the delta are due to use of an in-scene clay ROI endmember which is not representative of these materials, demonstrating that it is spectrally different from the clay-bearing deposits.